

Human $\alpha 6\beta 4$ nicotinic acetylcholine receptor: heterologous expression and agonist behavior provide insights into the immediate binding site

María Constanza Maldifassi^{1*}, Hugo Rego Campello³, Timothy Gallagher³, Henry A. Lester², Dennis A Dougherty¹

Affiliation

¹Division of Chemistry and Chemical Engineering, California Institute of Technology, Pasadena, California 91125, United States.

²Division of Biology and Biological Engineering, California Institute of Technology, Pasadena, California 91125, United States.

³School of Chemistry, University of Bristol, Bristol, BS8 1TS, United Kingdom

*Present affiliation: Institute of Biochemistry and Molecular Medicine, University of Bern, Bern 3012, Switzerland

Running title: Pharmacological characterization of the human $\alpha 6\beta 4$ nAChR

Corresponding author: María Constanza Maldifassi¹, PhD

Bühlstrasse 283012 Bern, Switzerland

E-mail: maria.maldifassi@ibmm.unibe.ch

Manuscript information:

Text pages: 26

Tables: 5 main tables and 3 supplementary tables

Number of figures: 4 main figures

Number of references: 39

Number of words in the Abstract: 147

Number of words in the Introduction: 737

Number of words in the Discussion: 397

Abbreviations:

ACh: acetylcholine

BARP: β -anchoring and regulatory protein

CCho: carbamylcholine

Cho: choline

Cyt: cytosine

Epi: epibatidine

Nic: nicotine

nAChRs: nicotinic acetylcholine receptors

Var: varenicline

VGCCs: voltage gated calcium channels

Abstract

Study of $\alpha 6\beta 4$ nicotinic acetylcholine receptors (nAChRs) as a pharmacological target has recently gained interest because of their involvement in analgesia, control of catecholamine secretion, dopaminergic pathways, and aversive pathways. However, an extensive characterization of the human $\alpha 6\beta 4$ nAChRs has been vitiated by technical difficulties resulting in poor receptor expression. In 2020, Knowland and collaborators identified BARP (β -anchoring and regulatory protein), a previously known voltage-gated calcium channel suppressor, as a novel human $\alpha 6\beta 4$ chaperone. Here we establish that co-expression of human BARP with human $\alpha 6\beta 4$ in *Xenopus* oocytes, resulted in the functional expression of human $\alpha 6\beta 4$ receptors with ACh-elicited currents that allow an in-depth characterization of the receptor using two electrode voltage-clamp electrophysiology together with diverse agonists and receptor mutations. We report: (1) an extended pharmacological characterization of the receptor, and (2) key residues for agonist-activity located in or near the first shell of the binding pocket.

Significance Statement

The human $\alpha 6\beta 4$ nicotinic acetylcholine receptor (nAChR) has attained increased interest because of its involvement in diverse physiological processes and diseases. Although recognized as a pharmacological target, development of specific agonists has been hampered by limited knowledge of its structural characteristics and by challenges in expressing the receptor. By including the chaperone BARP for enhanced expression and employing different ligands, we have studied the pharmacology of $\alpha 6\beta 4$, providing insight into receptor residues and structural requirements for ligands important to consider for agonist-induced activation.

Introduction

Nicotinic acetylcholine receptors (nAChRs) are pentameric ligand-activated ion channels (Le Novere and Changeux, 1995; Millar and Gotti, 2009) that have been extensively studied and are well-established pharmaceutical targets. Mammals have 16 distinct genes for nAChR subunits (Corradi and Bouzat, 2016), and each particular subunit contains four transmembrane helices, and extracellular N- and C-terminal domains. The agonist binding site of the receptor is located extracellularly at subunit interfaces, where the α subunit carries the principal component and (in heteropentameric nAChRs) the β subunit carries the complementary component (Corringer et al 2000; Grutter et al., 2004). The binding pocket contains a highly conserved core of aromatic amino acids, and contacts with these and other first-shell side chains and backbone atoms contribute to the pharmacological diversity of nAChRs (Corringer et al 2000; Grutter et al., 2004).

Interest in the human $\alpha 6^*$ ($\alpha 6$ -containing) nAChRs as a drug target arises because of their relevance in (i) analgesia through their expression in dorsal root ganglia (Hone et al., 2012; Knowland et al., 2020; Wieskopf et al., 2015), (ii) control of catecholamine secretion in chromaffin cells (Hernández-Vivanco et al., 2014; Pérez-Alvarez et al., 2012), (iii) both reward pathways (Wall et al., 2017) and degenerative disorders such as Parkinson's disease (Perez et al., 2010; Srinivasan et al., 2016), via expression in dopaminergic neurons, and (iv) expression in neurons of the medial habenula and interpeduncular nucleus (Henderson et al., 2014), which are implicated in aversive mood states such as addiction, anxiety, and depression (McLaughlin et al., 2017).

A special challenge associated with an $\alpha 6$ -subtype specific ligand centers on the close homology between the $\alpha 4$ and $\alpha 6$ subunits. Both are expressed in numerous neuronal types and several drugs previously considered selective for $\alpha 4^*$ nAChRs have now been shown to be comparably potent at $\alpha 6^*$ nAChRs (Quik and Wonnacott, 2011). Studies of heterologously expressed receptors that could address these challenges are further hampered by the fact that human $\alpha 6$ subunits produce very small

currents when expressed with various β subunits (Knowland et al., 2020; Letchworth and Whiteaker, 2011).

In many cases, accessory proteins interact with ion channel subunits within exocytotic pathways or at the plasma membrane of native cells, influencing the native current levels, kinetics, permeability, subunit stoichiometry, and even pharmacology. As such, co-expression of accessory proteins with various ion channels in heterologous systems is common practice (Lee et al., 2014; Li et al., 2017). For several nAChRs, including $\alpha 6$, co-expression of distinct chaperone proteins increases current amplitudes to levels where systematic study becomes possible in heterologous systems (Gu et al., 2019; Halevi et al., 2002; Knowland et al., 2020; Matta et al., 2017). In particular, the β -anchoring and regulatory protein (BARP), a transmembrane protein first recognized as a negative regulator of VGCCs (Beguin et al., 2014), has been demonstrated to enable ACh-elicited currents when co-injected in *Xenopus laevis* oocytes with human $\alpha 6$ and $\beta 4$ subunits (Knowland et al., 2020). However, no further characterization of the chaperoned receptor was provided. As such, a primary goal of this work was to address this deficiency.

Here, we provide information on the pharmacological characteristics and key residues in the binding site of the human $\alpha 6\beta 4$ receptor type. To circumvent the difficulties in expressing this receptor in heterologous systems, we used a dual approach with *Xenopus laevis* oocytes: the $\alpha 6$ subunit contained a hypersensitive serine mutation at the leucine 9' on M2; and we co-injected mRNA for human BARP (Knowland et al., 2020).

Given that a critical requirement in this area is the discovery of an $\alpha 6$ subtype selective agonist, we chose to evaluate cytosine (cytisinicline), which is a known $\alpha 4$ agonist and currently marketed (as Tabex) for smoking cessation. Further, we have an extensive ligand set based on modification of cytosine at either (or both) C(9) and C(10), where structural modification has already been demonstrated to impart differing selectivity across $\alpha 4$ -, $\alpha 3$ - and $\alpha 7$ -containing nAChRs. (Blom et al., 2019; Minguez-Viñas et al., 2021; Rego Campello et al., 2018; Slater et al., 2002). We have found that 9-bromocytosine derivatives are potent $\alpha 6\beta 4$ receptor agonists, with similar affinities as the

human $\alpha 7$ nAChR (Slater et al., 2002). Further, and in terms of receptor characteristics, our studies have highlighted those aromatic amino acids within the agonist binding site that are important for agonist activity. In combination, these results offer important new insights on the functional profile of the human $\alpha 6\beta 4$ receptor, knowledge that will impact the search for new and $\alpha 6$ subtype-specific receptor agonists.

Materials and Methods

Molecular Biology.

Obtention of mRNA and conventional mutagenesis was done as previously reported by our group (please see Blom et al., 2019 and references therein). In summary, circular DNA of human nAChR $\alpha 6$ subunit was in the pSP64T vector, and human BARP and $\beta 4$ subunits DNA were in a pGEMhe plasmid. cDNA in the pSP64T vector was linearized using the EcoRI enzyme, while cDNA in pGEMhe was linearized with restriction enzyme SbfI (New England Biolabs). Next, purified linear DNA (Qiaquick PCR Purification kit, Qiagen) was prepared by *in vitro* transcription, using the SP6 or T7 mMessage Machine kit (Ambion), accordingly. Afterwards, the mRNA was isolated using the RNeasy RNA purification kit according to the manufacturer's instructions (Qiagen) and was later quantified using UV-vis spectroscopy (NanoDrop 2000, ThermoFisher Scientific). Site-directed mutagenesis of specific residues was achieved by means of the Quick-Change protocol (Agilent Stratagene), and correspondingly all mutants were validated by sequencing. In our present work the human $\alpha 6$ subunit contains a background mutation in the transmembrane of TM2 helix termed $\alpha 6L9'S$. This mutation has been used previously by our group, and it is known to increase receptor expression and to lower whole cell EC_{50} values, which for convenience is referred to as a wild-type in the text (Post et al., 2015; Knox et al., 2022).

Xenopus laevis Oocyte Preparation and Injection.

Ion channel expression was carried out as formerly documented by our group (Xiu et al., 2009; Knox et al., 2022). Briefly, oocytes from stages V and VI were harvested, and afterwards injected with mRNAs, according to previously described protocols (Post et al., 2017). Because injecting a ratio of 1:1 is known to give rise to a mixed population of receptors (Moroni et al., 2006), and since we wanted to bias the receptor towards more α or more β in the pentamer, we used 1:10 or 10:1 injection

ratios of α : β subunits. Thus the α 6L9'S, β 4 and BARP mRNA were mixed in 1:10:5 or 10:1:5 ratio by mass. Each cell was injected with 50 ng mRNA in only a single injection. As can be observed in **Supplemental Table1**, the presence of BARP permits the finding of detectable currents and enables the calculation of the parameters of EC_{50} and Hill coefficients. After that, oocytes were incubated at 18 °C for 72-96 h before recording. Incubation media consisted in a ND96 solution (96 mM NaCl, 2 mM KCl, 1mM $MgCl_2$, 1.8 mM $CaCl_2$, 5 mM HEPES, pH 7.5) supplemented with 0.05 mg/mL gentamycin (Sigma), 2.5 mM sodium pyruvate (Acros Organics), 0.67 mM theophylline (Sigma), and 5% Horse Serum (Sigma).

Ligand Preparation.

(-)-Cytisine was a generous gift from Achieve Life Sciences. Synthesis of the C(9)/C(10) cytisine derivatives, and the corresponding structures, which were prepared from (-)-cytisine, have been described elsewhere (Rego Campello et al., 2018). All other agonists were purchased from Sigma.

Whole-Cell Electrophysiological Studies.

Two-electrode voltage clamp electrophysiology measurements were accomplished using the OpusXpress 6000A (Axon Instruments) at ambient temperature (20–25 °C) as previously described (Xiu et al., 2009; Knox et al., 2022). First, oocytes were impaled with 3 M KCl filled borosilicate glass pipettes ($R = 0.3\text{--}3.0\text{ M}\Omega$), and then clamped at a holding potential of -60 mV . As running buffer, a ND96 solution containing 1.8 mM of Ca^{2+} was used. Agonists were applied over 15 s, followed by a 2 min washout with buffer at a rate of 3 mL min^{-1} (chamber volume = $500\text{ }\mu\text{L}$). At least three different batches of oocytes were used for each mutant and agonist combination. Data was sampled at 50 Hz. Two-electrode voltage-clamp traces were processed using Clampfit 10.3 (Axon Instruments). Raw traces were filtered using a low-pass Gaussian filter at 5 Hz, followed by a subtraction of the average baseline current preceding agonist application. And normalized peak currents were averaged and fit to the Hill equation, $I_{\text{norm}} = 1/(1 + (EC_{50}/[\text{agonist}]^{nH})$ using Prism 8 (GraphPad Software, Inc.), where I_{norm} corresponds to the normalized peak current at a given agonist concentration, EC_{50} the agonist concentration that produces a half-maximum response, and nH the

Hill coefficient: where the peak currents obtained were always normalized to the maximum current observed for each corresponding oocyte. The EC_{50} obtained results are shown as mean \pm standard error of the mean (SEM).

RESULTS

Heterologous expression of human $\alpha 6\beta 4$ in *Xenopus* oocytes: pharmacological characterization

To pursue an investigation of the human $\alpha 6\beta 4$ receptor in *Xenopus* oocytes, we successfully combined (i) a L9'S mutation in the $\alpha 6$ M2 subunit, which is known to increase expression and conductance of nAChRs (Filatov and White, 1995; Fonck et al., 2005; Gleitsman et al., 2009; Xiu et al., 2009), with (ii) co-expression of BARP, the human $\alpha 6\beta 4$ chaperone (Knowland et al., 2020). All experiments described here involved the human $\alpha 6$ subunit containing the L9'S mutation, but for simplification this is referred to here as a "wild-type". Please observe in **Supplemental Table 1** how in the absence of this mutation, no detectable currents were obtained. In our initial studies, we used two $\alpha 6:\beta 4$:BARP mRNA injection ratios, corresponding to 1:10:5 and 10:1:5, keeping the total amount of mRNA constant at 50 ng in each cell. We first considered the agonists acetylcholine, nicotine, varenicline, cytosine, choline, carbamylcholine and epibatidine, a set of agonists already characterized at the rat $\alpha 6\beta 2$ receptor by our group (Post et al., 2015). In **Figure 1**, original currents traces for ACh (**A**) and cytosine (**B**) are shown. As can be observed in **Figure 1 C-D**, the dose-response relationship for each agonist was fitted by a single Hill term, indicating that likely only one population of receptors exists for each ratio injected. Interestingly, as shown in **Table 1**, for each agonist the EC_{50} values obtained for both injected ratios were similar. Based on previous experience with this expression strategy, we anticipated that such large variation in the injection ratio of $\alpha 6$ and $\beta 4$ would have created two stoichiometries of the receptor, one biased towards $\alpha 6$ and the other one to $\beta 4$ (Blom et al., 2019; Post et al., 2015). Based on the data in **Table 1**, we conclude that either the two limiting stoichiometries have very similar pharmacology or that an essentially homogenous population of functional receptors is produced and detected regardless of mRNA injection ratio. For all agonists

except ACh, the 10:1:5 ratio of $\alpha 6$ and $\beta 4$ consistently gave higher currents and, typically, larger Hill coefficients. As a consequence, we have employed the 10:1:5 ($\alpha 6$: $\beta 4$:BARP) ratio throughout our study, and based on these observations, we suggest that this produces the ($\alpha 6$)₃($\beta 4$)₂ receptor stoichiometry.

Concerning agonist potency, referring to EC₅₀ values, **Table 1** shows that choline is the least potent, followed by carbamylcholine, then acetylcholine and then cytosine, nicotine, varenicline, and the much more potent epibatidine. The order of potency (Epi > Cyt ~ Nic ~ Var ~ ACh > CCho > Cho) for these agonists resembles that found for the rat $\alpha 6\beta 2$ receptor (Post et al., 2015), and the potency for ACh is in the same range as reported for the rat $\alpha 6\beta 4$ (Wieskopf., 2015).

Relative efficacy studies for select agonists were carried out by applying two doses of ACh, followed by a dose of agonist at a concentration high enough to produce the maximal current in the dose-response curve, followed by two more applications of ACh, with appropriate wash out steps in between. The relative maximal current responses values are shown in **Supplemental Table 2** and are presented as relative to ACh. All agonists tested acted as partial agonists.

Investigating steric-tolerance in the human $\alpha 6\beta 4$ receptor binding site

In order to characterize more fully the binding site of the human $\alpha 6\beta 4$ receptor, we made use of a diverse set of cytosine derivatives, which have been functionalized at positions C(10) and C(9) (see caption in **Figure 2**). These structures have been used previously to explore structural elements within the ligand binding pocket of different nAChRs (Blom et al., 2019; Minguez-Viñas et al., 2021; Rego Campello et al., 2018). We selected ligands representing varying steric and electronic characteristics, and the concentration-response curves obtained are presented in **Figure 2**. **Table 2** lists the EC₅₀ fold shift relative to cytosine, where a shift of >2 was considered as a meaningful change.

As can be observed in **Table 2**, although most of the compounds tested had a modification of potency compared to cytosine, in general variation in EC₅₀ is smaller than seen in previous studies of other

nAChR subtypes. In particular, an increase of the size of the 10-substituent did not lead to a systematic decrease in potency as has been seen in other subtypes. Cytisine derivatives **6** ($R_1=H$; $R_2=Me$) and **3** ($R_1=H$; $R_2=Et$) had EC_{50} values comparable to cytisine **1**, the larger iPr derivative **5** showed a 9.6 fold shift, while the bulky, t-butyl variant **11** produced only a modest 4.4-fold shift. Perhaps surprisingly, compound **12** ($R_1=H$; $R_2=NHMe$) showed the largest (17.6 fold) shift in EC_{50} . Interestingly, ligands **10**, **13** and **16**, containing a 9-bromo moiety, demonstrated a substantial *decrease* of EC_{50} compared to the parent ligand **1**.

As a major goal of this work is to evaluate factors that distinguish different nAChR subtypes, **Table 3** compares the present results to previously published data from our group obtained for rat $\alpha 4\beta 2$ ($(\alpha 4)_2(\beta 2)_3$), rat $\alpha 4\beta 2$ (stoichiometry 3:2) and human $\alpha 3\beta 4$ (stoichiometry 2:3) receptors. While a general increase in EC_{50} is observed as the total volume of the agonist increases for $\alpha 4\beta 2$ (both stoichiometries), and $\alpha 3\beta 4$ receptors, the overall effect is substantially smaller with the $\alpha 6\beta 4$ receptor. This suggests that other receptor subtypes have a more compact binding pocket than $\alpha 6\beta 4$. To further probe this effect, we focused on the steric demand of 10-substituted cytisines using ligands **6**, **3**, **4**, **5** and **11** displaying a progressive *increase* in substituent size ($Me < Et < C(CH_3)=CH_2 < iPr < t-Bu$) but, given the similarity of the alkyl/alkenyl residues present, where no variation in electronic effects was expected.

We also set to determine the origin of the differing responses to the ligand steric effects described above. As the $\alpha 3\beta 4$ and $\alpha 6\beta 4$ subtypes share the same complementary component of the binding site, and since the aromatic binding site residues within the principal component are identical between the diverse α subtypes, we focused on the residues near Trp179 (TrpB) and Tyr227 (TyrC2); both residues are known to be important for cytisine agonist action (Blom et al., 2019; Tavares et al., 2012). Potentially influential residues (shown in yellow in the sequence alignment of **Figure 4**) were identified in loops B and C of the $\alpha 6$ residue and mutated to the homologous residues located in the $\alpha 3$ subunit. Mutations studied were T180S, T228P and N221E. A more detailed localization of these residues and the mutated counterparts can be observed in **Figure 3**. Here, **Figure 4** shows the plot of shifts in agonist potency (EC_{50}) versus total volume of the ligand in \AA^3 for each mutant, with a larger

slope implying a greater sensitivity to steric demands, and **Supplemental Table 3** shows the results obtained. When the Thr180 residue is mutated to Ser, this resulted in a *decrease* of affinity for almost all compounds tested, though not statistically significant. Additionally, the T180S mutation did increase EC₅₀ for cytosine. The residue adjacent to TyrC2 is Thr for the $\alpha 6$ subunit, but Pro within every other subunit except for the muscle type $\alpha 1$ subunit. Replacement of Thr228 by Pro in the $\alpha 6\beta 4$ receptor led to only a moderate increase of affinity for bulky substitutions compared to cytosine. Given that substituting Thr to Pro is arguably a more dramatic perturbation, the overall effect observed was smaller than that for the more subtle Thr-Ser mutation adjacent to TrpB (**Supplemental Table 3**). We also considered the residue located immediately prior to the vicinal cysteines in loop C, which through interactions with residues located on loop F may be relevant in defining the size of the binding pocket (Gharpure et al., 2019). In both the $\alpha 6$ and $\alpha 3$ subunits this residue is Asn but in $\alpha 4$ is a Glu (see **Figure 3C** for localization and the alignment in **Figure 4**). When we mutated Asn221 to Glu (N221E), as seen in **Figure 4**, we observed an increase in the apparent affinity for cytosine. Remarkably, a considerable decrease in affinity is observed for all derivatives tested compared to cytosine, with this mutation rendering the receptor more bulk-intolerant, which is supported by an apparent increase in the slope of the mutant receptor. Overall, our data points to these residues (T180, T228 and N221) as important determinants for the affinity of cytosine (and C(10) cytosine derivatives) in the $\alpha 6\beta 4$ receptor, with steric effects playing some role.

9-Bromocytosine derivatives: potent agonists at $\alpha 6\beta 4$ receptors

Electrophilic bromination of cytosine occurs predominantly at C(9) and is known to result in an increase of agonist activity in nAChRs (Abin-Carriquiry et al., 2010; Blom et al., 2019; Houlihan et al., 2001; Slater et al., 2002). In $\alpha 6\beta 4$ receptors, cytosine ligands incorporating a C(9) bromo moiety led to a substantial decrease of EC₅₀, as shown in **Table 2** and **Table 4**. The increased potency, evident with 9-bromocytosine **16**, was substantial and maintained in combination with C(10) substitution (NH₂ or Et **10** and **13** respectively). However, this was attenuated in the case of ligand **14**

bearing a 10-NHMe substitution. This pattern has been seen before, and we previously speculated that this variance arises as a result of different conformational preferences of the C(10) substituents (Blom et al., 2019). Furthermore, if we compare potency shifts due to the addition of a 9-Br group with the effects obtained at $\alpha 4\beta 2$ and $\alpha 3\beta 4$ receptors as seen in **Table 3**, we observe that the *increase in potency* is generally greater for the $\alpha 6\beta 4$ receptor.

Several reports have proposed that a C(9)-Br substituent in cytosine may interact with Val111 and Phe119 residues located on the complementary face of the $\alpha 4\beta 2$ receptor (Abin-Carriquiri et al., 2010; Rego Campello et al., 2018). Consequently, we wondered whether mutating the equivalent $\beta 4$ residues, Ile113 and Leu121, which are represented in **Figure 3C**, would also affect the potency for 9-bromocytosines. As shown in **Table 4**, the I113V $\beta 4$ mutant had little impact on EC₅₀ for cytosine or the three 9-bromo variants (**10**, **13** and **16**) examined. Thus, the “bromo effect” discussed above is still present in the Val mutant. With ligands **3** and **9** (which correspond to **13** and **10** but lacking the 9-Br component), a 2 to 3 fold decrease in potency was observed in the I113V mutant. This may indicate that the mutation causes a re-alignment of the agonist and thus alters substituent-receptor interactions at the complementary binding face. Mutation of Ile113 to Ala led to a decrease in potency for cytosine, while with ligands **13** and **16** the relative potentiation effect of Br was increased. Finally, mutation of $\beta 4$ -Leu121 residue to Ala (**Table 4**) had minimal impact on potency except for ligand **9** (R₂ = NH₂), where we observed a very substantial *reduction* in potency.

Relative efficacy studies were conducted also on most of the Br-containing agonists studied. As can be observed in **Supplemental Table 2**, in general cytosine and 10-substituted variants act to a different extent as partial agonists at $\alpha 6\beta 4$ receptors. Exceptions are ligands **16** and **13** carrying a 9-bromo residue which are more efficacious than cytosine **1** or the desbromo variant **3**. Again, this is in line with previously published results that demonstrated that C(9)-halogenation of cytosine favored nAChRs receptor activation (Slater et al., 2002).

Characteristic aromatic residues in the binding pocket: Relevance for agonist effects

The orthosteric binding site in nicotinic receptors is located in the extracellular domain at the interface between subunits. Here, highly conserved aromatic residues located on loops A (Tyr122, TyrA), B (Trp179, TrpB), C (two Tyr: C1-220 and C2-227) and D (Trp85, TrpD) form a well-documented aromatic ‘box’ wherein agonists are nested (see **Figure 3C** for relative organization of this site). To determine the functional significance of these aromatic amino acids in the $\alpha 6\beta 4$ receptor, each residue was mutated to Ala. As shown in **Table 5**, the mutation of TrpD to Ala resulted in an apparent small increase in affinity for ACh and cytosine. Alanine mutation of TyrC2, a residue known to interact with cytosine through a cation- π interaction in the $\alpha 4\beta 2$ receptors (Blom et al., 2019), led to no measurable agonist response with either ACh or cytosine. Additionally, the importance of the phenol residue of TyrC2 was assessed by mutation to Phe. As shown in **Table 5**, this mutation barely changes the EC_{50} for ACh, however, the OH of tyrosine is essential for the agonist effects of cytosine, an effect previously observed for the $\alpha 4\beta 2$ receptor (Blom et al., 2019). Mutation of TrpB to Ala led to loss of potency for both ACh and cytosine, but this was more pronounced for ACh. Interestingly, though, mutation of this key residue did not render the receptor completely unresponsive to either agonist, as would be expected as a consequence of the involvement of a cation- π interaction determinant for agonist binding. Finally, we investigated the role of TyrA. Here mutation to Ala resulted in similar decreases of potency for ACh and cytosine. Our results here show that of the residues investigated, mutation of TyrC2 had the most deleterious effects upon agonist-induced activation in human $\alpha 6\beta 4$ receptor. This result, highlighting a critical role for TyrC2, parallels previous observations that determined experimentally that cytosine is able to interact with this residue through a combination of both cation- π effects and phenol-based hydrogen bond interactions in different nAChRs (Abin-Carriquiry et al., 2010; Blom et al., 2019; Rego Campello et al., 2018).

DISCUSSION

In the present work we sought to characterize the pharmacology of the $\alpha 6\beta 4$ nAChR, an interesting subtype of this important class of receptors. The first challenge was to develop expression conditions in *Xenopus* oocytes that produced adequate quantities of receptor for detailed characterization. Two modifications of standard mRNA injection produced the desired result: incorporation of an L9'S mutation in the $\alpha 6$ subunit and coexpression of the chaperone BARP. In this way, consistent expression of a homogeneous population of receptors was achieved.

Against a range of agonists, the $\alpha 6\beta 4$ receptor showed typical responses. However, when probed more thoroughly using an array of systematically-modified cytosine derivatives, meaningful differences between $\alpha 6\beta 4$ and other subtypes were seen. Most tellingly, the $\alpha 6\beta 4$ agonist binding site is less sensitive to increasing steric bulk on the cytosine ligand than other receptor subtypes. This suggests a more open, ligand volume-tolerant agonist binding site in $\alpha 6\beta 4$. Several residues adjacent to known contributors to the agonist binding site were evaluated as possible determinants of this more open structure, but no clear trends emerged. In contrast, the $\alpha 6\beta 4$ subtype is more sensitive to substitution by Br at C(9) of cytosine, with Br-substituted derivatives (such as **10**, **13** and **14**) showing substantial increases in potency.

A number of aromatic (Tyr and Trp) residues are known to define a large part of the agonist binding site of nAChRs. We mutated these residues to Ala to probe their role in $\alpha 6\beta 4$. The TrpD/Ala mutation had a small effect, while the TyrC2/Ala mutant was not responsive to ACh or cytosine. It has been established that TyrC2 makes a strong cation- π interaction with cytosine. Interestingly, the TyrC2/Phe mutation had no effect on ACh potency, but was strongly perturbative for cytosine, suggesting a role for the OH of TyrC2 in binding cytosine. When TrpB, the near universal cation- π binding site in

nAChRs, is mutated to Ala, agonist potency is substantially impacted, but, interestingly, the mutant receptor is not totally unresponsive to either ACh or cytosine. Finally, the TyrA/Ala mutation showed decreased potency for both ACh and cytosine. These results point to a perhaps more important role for TyrC2 in binding cytosine than typically seen at other receptor/agonist combinations.

Overall, our results reveal similarities, but also interesting differences, between $\alpha 6\beta 4$ and other nAChR subtypes. It is hoped that such insights will be of value to efforts to develop selective agonists/antagonists for this important nAChR subtype.

Acknowledgments

We here like to thank Jonathan Wang and Purnima Deshpande for the furnishing of the *Xenopus* oocytes.

Data Availability Statement

The authors declare that all the data supporting the findings of this study are available within the paper and its **Supplemental Data**.

Authorship Contributions

Participated in research design: Maldifassi MC, Dougherty DA

Conducted experiments: Maldifassi MC

Contributed new reagents or analytic tools: Gallagher T, Rego Campello H

Performed data analysis: Maldifassi MC, Dougherty DA, Lester HA

Wrote or contributed to the writing of the manuscript: Maldifassi MC, Dougherty DA, Lester HA, Gallagher T, Rego Campello H

Footnotes

This work was supported by The Regents of the University of California, Research Grants Program Office, Tobacco Related Disease Research Program (Grant No. T29IR0455 to D.A.D.). The authors declare that they have no conflict of interest with the contents of this article.

REFERENCES

- Abin-Carriquiry JA, Zunini MP, Cassels BK, Wonnacott S, and Dajas F (2010) In silico characterization of cytosinoids docked into an acetylcholine binding protein. *Bioorg Med Chem Lett* 12:3683-3687.
- Béguin P, Nagashima K, Mahalakshmi RN, Vigot R, Matsunaga A, Miki T, Ng MY, Ng YJ, Lim CH, Tay HS, Hwang LA, Firsov D, Tang BL, Inagaki N, Mori Y, Seino S, Launey T, and Hunziker W (2014) BARP suppresses voltage-gated calcium channel activity and Ca^{2+} -evoked exocytosis. *J Cell Biol* 205:233-249.
- Blom AEM, Campello HR, Lester HA, Gallagher T, and Dougherty DA (2019) Probing Binding Interactions of Cytisine Derivatives to the $\alpha 4\beta 2$ Nicotinic Acetylcholine Receptor. *J Am Chem Soc* 141:15840-15849.
- Corradi J, and Bouzat C (2016) Understanding the Bases of Function and Modulation of $\alpha 7$ Nicotinic Receptors: Implications for Drug Discovery. *Mol Pharmacol* 90:288-299.
- Corringer PJ, Le Novère N, and Changeux JP (2000) Nicotinic receptors at the amino acid level. *Annu Rev Pharmacol Toxicol* 40:431-458.
- Filatov GN, and White MM (1995) The role of conserved leucines in the M2 domain of the acetylcholine receptor in channel gating. *Mol Pharmacol* 48:379-384.
- Fonck C, Cohen BN, Nashmi R, Whiteaker P, Wagenaar DA, Rodrigues-Pinguet N, Deshpande P, McKinney S, Kwoh S, Munoz J, Labarca C, Collins AC, Marks MJ, and Lester HA (2005) Novel seizure phenotype and sleep disruptions in knock-in mice with hypersensitive $\alpha 4^*$ nicotinic receptors. *J Neurosci* 25:11396-11411.

Gharpure A, Teng J, Zhuang Y, Noviello CM, Walsh RM Jr, Cabuco R, Howard RJ, Zaveri NT, Lindahl E, and Hibbs RE (2019) Agonist Selectivity and Ion Permeation in the $\alpha 3\beta 4$ Ganglionic Nicotinic Receptor. *Neuron* 104:501-511.

Gleitsman KR, Shanata JA, Frazier SJ, Lester HA, and Dougherty DA (2009) Long-range coupling in an allosteric receptor revealed by mutant cycle analysis. *Biophys J* 96:3168-3178.

Grutter T, Le Novère N, and Changeux JP (2004) Rational understanding of nicotinic receptors drug binding. *Curr Top Med Chem* 4:645-650.

Gu S, Matta JA, Davini WB, Dawe GB, Lord B, and Brecht DS (2019) $\alpha 6$ -Containing Nicotinic Acetylcholine Receptor Reconstitution Involves Mechanistically Distinct Accessory Components. *Cell Rep* 26:866-874.

Halevi S, McKay J, Palfreyman M, Yassin L, Eshel M, Jorgensen E, and Treinin M (2002) The C. elegans ric-3 gene is required for maturation of nicotinic acetylcholine receptors. *EMBO J* 21:1012-1020.

Henderson BJ, Srinivasan R, Nichols WA, Dilworth CN, Gutierrez DF, Mackey ED, McKinney S, Drenan RM, Richards CI, and Lester HA (2014) Nicotine exploits a COPI-mediated process for chaperone-mediated up-regulation of its receptors. *J Gen Physiol* 143:51-66.

Hernández-Vivanco A, Hone AJ, Scadden ML, Carmona-Hidalgo B, McIntosh JM, Albillos A (2014) Monkey adrenal chromaffin cells express $\alpha 6\beta 4^*$ nicotinic acetylcholine receptors. *PLoS One* 9:e94142.

Hone AJ, Meyer EL, McIntyre M, and McIntosh JM (2012) Nicotinic acetylcholine receptors in dorsal root ganglion neurons include the $\alpha 6\beta 4^*$ subtype. *FASEB J* 26:917-926.

Houlihan LM, Slater Y, Guerra DL, Peng JH, Kuo YP, Lukas RJ, Cassels BK, and Bermudez I (2001) Activity of cytosine and its brominated isosteres on recombinant human $\alpha 7$, $\alpha 4\beta 2$ and $\alpha 4\beta 4$ nicotinic acetylcholine receptors. *J Neurochem* 78:1029-1043.

- Knowland D, Gu S, Eckert WA 3rd, Dawe GB, Matta JA, Limberis J, Wickenden AD, Bhattacharya A, and Brecht DS (2020) Functional $\alpha 6\beta 4$ acetylcholine receptor expression enables pharmacological testing of nicotinic agonists with analgesic properties. *J Clin Invest* 130:6158-6170.
- Knox HJ, Rego Campello H, Lester HA, Gallagher T, Dougherty DA (2022) Characterization of binding site interactions and selectivity principles in the $\alpha 3\beta 4$ nicotinic acetylcholine receptor. *J Am Chem Soc* 144:16101-16117.
- Le Novère N, and Changeux JP (1995) Molecular evolution of the nicotinic acetylcholine receptor: an example of multigene family in excitable cells. *J Mol Evol* 40:155-172.
- Lee A, Fakler B, Kaczmarek LK, and Isom LL (2014) More than a pore: ion channel signaling complexes. *J Neurosci* 34:15159-15169.
- Letchworth SR, and Whiteaker P (2011) Progress and challenges in the study of $\alpha 6$ -containing nicotinic acetylcholine receptors. *Biochem Pharmacol* 82:862-872.
- Li K, Jiang Q, Bai X, Yang YF, Ruan MY, and Cai SQ (2017) Tetrameric Assembly of K(+) Channels Requires ER-Located Chaperone Proteins. *Mol Cell* 65:52-65.
- Matta JA, Gu S, Davini WB, Lord B, Siuda ER, Harrington AW, and Brecht DS (2017) NACHO Mediates Nicotinic Acetylcholine Receptor Function throughout the Brain. *Cell Rep* 19:688-696.
- McLaughlin I, Dani JA, De Biasi M (2011) The medial habenula and interpeduncular nucleus circuitry is critical in addiction, anxiety, and mood regulation. *J Neurochem* 142:130-143.
- Millar NS, and Gotti C (2009) Diversity of vertebrate nicotinic acetylcholine receptors. *Neuropharmacology* 56:237-246.
- Minguez-Viñas T, Nielsen BE, Shoemark DK, Gotti C, Sessions RB, Mulholland AJ, Bouzat C, Wonnacott S, Gallagher T, Bermudez I, and Oliveira AS (2021) A conserved arginine with non-conserved function is a key determinant of agonist selectivity in $\alpha 7$ nicotinic ACh receptors. *Br J Pharmacol* 178:1651-1668.

- Moroni M, Zwart R, Sher E, Cassels BK, and Bermudez I (2006) $\alpha 4\beta 2$ Nicotinic Receptors with High and Low Acetylcholine Sensitivity: Pharmacology, Stoichiometry, and Sensitivity to Long-Term Exposure to Nicotine. *Mol Pharmacol* 70:755-768.
- Perez XA, Bordia T, McIntosh JM, and Quik M (2010) $\alpha 6\beta 2^*$ and $\alpha 4\beta 2^*$ nicotinic receptors both regulate dopamine signaling with increased nigrostriatal damage: relevance to Parkinson's disease. *Mol Pharmacol* 78:971-980.
- Pérez-Alvarez A, Hernández-Vivanco A, McIntosh JM, and Albillos A (2012) Native $\alpha 6\beta 4^*$ nicotinic receptors control exocytosis in human chromaffin cells of the adrenal gland. *FASEB J* 26:346-354.
- Post MR, Limapichat W, Lester HA, and Dougherty DA (2015) Heterologous expression and nonsense suppression provide insights into agonist behavior at $\alpha 6\beta 2$ nicotinic acetylcholine receptors. *Neuropharmacology* 97:376-382.
- Post MR, Tender GS, Lester HA, and Dougherty DA (2017) Secondary Ammonium Agonists Make Dual Cation- π Interactions in $\alpha 4\beta 2$ Nicotinic Receptors. *eNeuro* 4:ENEURO.0032-17.2017.
- Quik M, Wonnacott S (2011) $\alpha 6\beta 2^*$ and $\alpha 4\beta 2^*$ nicotinic acetylcholine receptors as drug targets for Parkinson's disease. *Pharmacol Rev* 63:938-966.
- Rego Campello H, Del Villar SG, Honraedt A, Minguez T, Oliveira ASF, Ranaghan KE, Shoemark DK, Bermudez I, Gotti C, Sessions R, Mulholland AJ, Wonnacott S, and Gallagher T (2018) Unlocking Nicotinic Selectivity via Direct C–H Functionalization of (–) Cytisine. *Chem* 4:1710-1725.
- Slater YE, Houlihan LM, Maskell PD, Exley R, Bermúdez I, Lukas RJ, Valdivia AC, and Cassels BK (2002) Halogenated cytosine derivatives as agonists at human neuronal nicotinic acetylcholine receptor subtypes. *Neuropharmacology* 44:503-515.
- Srinivasan R, Henley BM, Henderson BJ, Indersmitten T, Cohen BN, Kim CH, McKinney S, Deshpande P, Xiao C, and Lester HA (2016) Smoking-Relevant Nicotine Concentration Attenuates the Unfolded Protein Response in Dopaminergic Neurons. *J Neurosci* 36:65-79.

Tavares Xda S, Blum AP, Nakamura DT, Puskar NL, Shanata JA, Lester HA, and Dougherty DA (2012) Variations in binding among several agonists at two stoichiometries of the neuronal, $\alpha 4\beta 2$ nicotinic receptor. *J Am Chem Soc* 134:11474-11480.

Wall TR, Henderson BJ, Voren G, Wageman CR, Deshpande P, Cohen BN, Grady SR, Marks MJ, Yohannes D, Kenny PJ, Bencherif M, and Lester HA (2017) TC299423, a Novel Agonist for Nicotinic Acetylcholine Receptors. *Front Pharmacol* doi: 10.3389/fphar.2017.00641.

Wieskopf JS, Mathur J, Limapichat W, Post MR, Al-Qazzaz M, Sorge RE, Martin LJ, Zaykin DV, Smith SB, Freitas K, Austin JS, Dai F, Zhang J, Marcovitz J, Tuttle AH, Slepian PM, Clarke S, Drenan RM, Janes J, Al Sharari S, Segall SK, Aasvang EK, Lai W, Bittner R, Richards CI, Slade GD, Kehlet H, Walker J, Maskos U, Changeux JP, Devor M, Maixner W, Diatchenko L, Belfer I, Dougherty DA, Su AI, Lummis SC, Imad Damaj M, Lester HA, Patapoutian A, and Mogil JS (2015) The nicotinic $\alpha 6$ subunit gene determines variability in chronic pain sensitivity via cross-inhibition of P2X2/3 receptors. *Sci Transl Med* 7:287ra72.

Xiu X, Puskar NL, Shanata JA, Lester HA, and Dougherty DA (2009) Nicotine binding to brain receptors requires a strong cation-pi interaction. *Nature* 458:534-537.

FIGURE LEGENDS

Figure 1: Examples of the human $\alpha 6\beta 4$ response to ACh (**A**) and cytisine (**B**). Oocytes were injected with of $\alpha 6\beta 4$:BAP mRNAs in a ratio of 10:1:5. Bars above the traces indicate the timing of the agonist applications and the numbers above the bars give the agonist concentrations. Inward current responses are shown as downward deflections of the trace. (**C-D**) Concentration-response relations for diverse nicotinic agonists measured for human $\alpha 6\beta 4$ receptors expressed in *Xenopus laevis* oocytes. Oocytes were injected with a mRNA ratio of 10:1:5 (**C**) or 1:10:5 (**D**), corresponding to $\alpha 6\beta 4$:BAP. Agonist abbreviations are as follows; ACh: acetylcholine; CYT: cytisine; VAR: varenicline; EPI: epibatidine; CHO: choline; CCHO: carbamylcholine; NIC: nicotine. Curved lines are fits to the Hill equation and are monophasic. Data points are means \pm SD. Please refer to **Table 1** for the cell sample size, EC_{50} , and Hill coefficients for the various agonists.

Figure 2: Human $\alpha 6\beta 4$ concentration-response relations for cytisine and the cytisine derivatives tested in this study. Lines are fits to the Hill equation. Inset shows the structural formula of cytisine. R1 and R2 indicate positions of C(9) and C(10) substituents, respectively. R1 is H for single substituents, whereas R1 is Br for R1/R2 double substituents. Data points are mean \pm SD. See **Table 2** for the number of cells tested, EC_{50} s and Hill coefficients for the concentration-response relation of the compounds.

Figure 3: A schematic view of some of the functionally relevant residues probed in this study. The image depicts the crystalized $\alpha 3\beta 4$ nAChR binding site with nicotine highlighted in pink (PDB ID:6PV7, Garpure et al., 2019). (**A-C**) Amino acids from the principal $\alpha 3$ side are shown in cyan, and from the $\beta 4$ side are in violet. Residues relevant for this study are in brown, namely S180 (**A**), P228

(B), and E221 (C). (D) Amino acids from the principal $\alpha 3$ side are shown in brown, and from the $\beta 4$ side are in green. Residues that contribute to the aromatic box and important for interactions are labeled. Blue denotes H bonds, and cation- π interactions are in the residues corresponding color.

Figure 4: Non-aromatic residues located at the binding site influence the tolerance of the human $\alpha 6\beta 4$ receptor for bulky agonists. (A) Effects of mutations of key residues of the $\alpha 6$ subunit on the relationship between ligand volume and shifts in relative potency. Total ligand volume in \AA^3 was plotted against the shift in the EC_{50} for each substituent relative to cytosine for the human $\alpha 6\beta 4$ receptor. Only derivatives containing substituents that increased agonist volume without other alterations in their chemical properties were included in this analysis. Data points are means \pm SD. * $p < 0.05$ compared to the WT $\alpha 6\beta 4$ obtained slope, t-test. (B) Sequence alignment for amino acids located at Loop A, B and C in the binding site of various nAChR subunits from human origin. Residues we mutated are highlighted in yellow, and residues that are part of the aromatic box are highlighted in blue.

TABLES

Table 1: Estimated μM EC_{50} values and Hill coefficients for diverse nicotinic agonists tested against human $\alpha 6\beta 4$ receptors.

Agonist	Stoichiometry	EC_{50}	$\text{pEC}_{50} (\text{CI}_{95\%})^a$	Hill	n^b	$\text{I}_{\text{max}} \mu\text{A}$
ACh	1:10:5	0.6 ± 0.2	0.2(0.2 to 0.3)	1.2 ± 0.5	15	0.37-2.46
ACh	10:1:5	1.6 ± 1.0	-0.2(-0.1 to -0.2)	1.2 ± 0.7	11	0.12-0.77
Cyt	1:10:5	0.6 ± 0.2	0.2(0.1 to 0.3)	1.4 ± 0.7	6	0.07-0.62
Cyt	10:1:5	0.5 ± 0.2	0.3(0.2 to 0.3)	1.4 ± 0.5	10	0.22-1.27
Epi	1:10:5	1.6 ± 0.5^c	3.0(2.8 to 3.1)	1.4 ± 0.7	12	0.07-0.64
Epi	10:1:5	4.4 ± 1.0^c	2.4(2.3 to 2.4)	2.5 ± 1.0	7	0.27-1.32
Var	1:10:5	0.3 ± 0.1	0.5(0.6 to 0.4)	1.4 ± 0.5	7	0.06-0.56
Var	10:1:5	0.1 ± 0.0	0.9(0.9 to 1.0)	2.1 ± 0.7	7	0.07-2.06
Cho	1:10:5	84.1 ± 36	-2.0(1.5 to 2.1)	1.0 ± 0.5	7	0.09-0.26
Cho	10:1:5	89.9 ± 23	-2.0(-1.9 to -2)	1.7 ± 0.8	9	1.02-5.05
CCho	1:10:5	4.4 ± 2.5	-0.6(-0.4 to -0.6)	1.1 ± 0.5	9	0.10-0.25
CCho	10:1:5	3.1 ± 0.8	-0.5(-0.4 to -0.6)	2.1 ± 1.4	9	0.47-13.81
Nic	1:10:5	0.2 ± 0.1	0.7(0.4 to 0.6)	1.7 ± 1.0	4	0.05-0.09
Nic	10:1:5	0.3 ± 0.1	0.5(0.4 to 0.6)	1.8 ± 0.9	10	4.86-18.54

The human $\alpha 6\beta 4$ receptor was expressed in *Xenopus laevis* oocytes, where $\alpha 6\beta 4$:BAPC mRNA injection ratio varied from 1:10:5 to 10:1:5. Agonist responses were measured using two-electrode voltage clamp electrophysiology. Monophasic concentration-response curves were fitted to the Hill equation. Agonist EC_{50} values are shown as Mean \pm SD. ^a pEC_{50} corresponds to $(-1 * \log \text{EC}_{50})$. ^b corresponds to the number of cells. ^c EC_{50} values in nM concentrations.

Table 2: The μM EC_{50} values and Hill coefficients of diverse cytosine derivatives tested with human $\alpha 6\beta 4$ receptors.

	Derivative	$\text{EC}_{50}^{\text{a}}$	$\text{pEC}_{50}(\text{CI}_{95\%})^{\text{b}}$	Hill	n ^c	Imax μA	Fold shift ^f
1	Cytisine	0.5 \pm 0.2	0.3(0.2 to 0.3)	1.4 \pm 0.2	10	0.22-1.27	1
2	F	2.7 \pm 0.6 ^{***}	-0.4(-0.6 to -0.1)	1.3 \pm 0.9	9	0.08-1.43	5.4
3	Et	0.6 \pm 0.3	0.2(0.1 to 0.3)	2.0 \pm 0.4	9	0.11-1.13	1.2
4	C(CH ₃)=CH ₂	2.4 \pm 0.6 ^{***}	-0.4(0.3 to 0.4)	2.0 \pm 0.5	12	0.07-1.55	4.8
5	iPr	4.8 \pm 0.5 ^{***}	-0.7(0.6 to 0.7)	1.4 \pm 0.9	6	0.05-0.73	9.6
6	Me	0.7 \pm 0.3	0.2(0.1 to 0.2)	1.8 \pm 0.4	8	0.08-1.58	1.4
7	Tolyl	0.4 \pm 0.2	0.4(0.3 to 0.5)	2.1 \pm 0.4	6	0.07-1.43	0.8
8	OMe	1.4 \pm 0.3 ^{***}	-0.1(-0.0 to -0.3)	2.0 \pm 0.5	6	0.05-0.16	2.8
9	NH ₂	1.5 \pm 0.8 ^{**}	-0.2(-0.1 to -0.3)	1.2 \pm 0.4	9	0.06-0.21	3
10	Br/NH ₂	30 \pm 7.0 ^{d***}	1.6(1.4 to 1.7)	1.9 \pm 0.9	7	0.05-0.86	0.06
11	tBu	2.2 \pm 0.5 ^{***}	-0.3(-0.3 to -0.4)	1.7 \pm 0.5	7	0.05-0.12	4.4
12	NHMe	8.8 \pm 2.3 ^{***}	-0.9(-0.8 to -1.0)	1.2 \pm 0.3	7	0.10-0.45	17.6
13	Br/Et	30 \pm 6.4 ^{d***}	2.0(1.5 to 2.0)	1.6 \pm 0.7	8	0.06-0.22	0.06
14	Br/NHMe	3.8 \pm 1.1 ^{***}	-0.6(-0.5 to -0.7)	1.1 \pm 0.4	7	0.06-0.22	7.6
15	CF ₃	4.0 \pm 1.0 ^{***}	-0.6(-0.4 to -0.7)	1.3 \pm 0.4	6	0.05-0.93	8
16	9-Br	13 \pm 3.4 ^d	2.0(1.8 to 2.0)	1.4 \pm 0.5	10	0.06-0.21	0.02

The human $\alpha 6\beta 4$ receptor was expressed in *Xenopus laevis* oocytes, and for this set of experiments the $\alpha 6\beta 4$:BAP mRNA injection ratio was 10:1:5. Agonist responses were measured as detailed in methods. Concentration-response relations were monophasic and fitted to the Hill equation. Agonist EC_{50} values are represented as Mean \pm SD. ^ffold shifts compared to cytosine. ^a ^{**} $p < 0.01$, ^{***} $p < 0.001$

compared to cytosine EC₅₀, t-test; ^bpEC₅₀ corresponds to (-1*logEC₅₀); ^c corresponds to the number of cells;

^dEC₅₀ values in nM concentrations.

Table 3: Comparison of folds shifts versus ligand volume for cytosine and the derivatives studied obtained in the human $\alpha 6\beta 4$, rat $\alpha 4\beta 2$ (stoichiometry 2:3), rat $\alpha 4\beta 2$ (stoichiometry 3:2) and human $\alpha 3\beta 4$ (stoichiometry 2:3) receptors.

	Derivative	$\alpha 6\beta 4$	$\alpha 3\beta 4$ (2:3)I	$\alpha 4\beta 2$ (3:2)*	$\alpha 4\beta 2$ (2:3)* I	Volume (Å)*
1	Cytosine	1	1	1	1	198
2	F	5.4	13	1.2	1.3	203
9	NH ₂	3	36	66	5.4	208
6	Me	1.4	5.8	1.9	2.3	216
8	OMe	2.8	15	17	14	225
10	Br/NH ₂	0.06	0.19	0.3	0.23	226
12	NHMe	17.6	13	19	44	228
15	CF ₃	8	5.8	17	18	230
3	Et	1	15	16	4.3	234
14	Br/NHMe	7.6	28	46	37	246
4	C(CH ₃)=CH ₂	4.8	22	44	17	249
5	iPr	9.6	12	42	7.7	252
13	Br/Et	0.06	0.039	0.38	0.21	253
11	tBu	4.4	25	35	7	270

Entries in the middle four columns are the EC₅₀ for the derivatives divided by that for cytosine.

Ligand volumes were taken from a previously publication (Blom et al., 2019). I data obtained from

Knox et al., 2022; * Data obtained from Blom et al., 2019.

Table 4: The μM EC_{50} values and Hill coefficients for cytosine and the 9-Br halogenated derivatives measured for the WT and mutated $\alpha 6\beta 4$ receptors.

	$\alpha 6\beta 4$	$\text{EC}_{50}^{\text{a}}$	$\text{pEC}_{50} (\text{CI}_{95\%})^{\text{b}}$	Hill	n^{c}	$\text{Imax } \mu\text{A}$	Fold shift
1	Cytosine	0.5 ± 0.2	$0.3(0.2 \text{ to } 0.3)$	1.4 ± 0.2	10	0.22-1.27	1
16	Br(9)	$13 \pm 3.4^{\text{d***}}$	$2.0(1.8 \text{ to } 2.0)$	1.4 ± 0.5	10	0.06-0.21	0.02
3	Et	0.6 ± 0.3	$0.2(0.1 \text{ to } 0.3)$	2.0 ± 0.4	9	0.11-1.13	1
13	Br/Et	$30 \pm 6.4^{\text{d***}}$	$2.0(1.5 \text{ to } 2.0)$	1.6 ± 0.7	8	0.06-0.22	0.06
9	NH_2	$1.5 \pm 0.8^{**}$	$-0.2(-0.1 \text{ to } -0.3)$	1.2 ± 0.4	9	0.06-0.21	3
10	Br/ NH_2	$30 \pm 7.0^{\text{d***}}$	$1.6(1.4 \text{ to } 1.7)$	1.9 ± 0.9	7	0.05-0.86	0.06
	$\alpha 6\beta 4\text{I113V}$	$\text{EC}_{50}^{\text{a}}$	$\text{pEC}_{50} (\text{CI}_{95\%})^{\text{b}}$	Hill	n^{c}	$\text{Imax } \mu\text{A}$	Fold shift
1	Cytosine	0.9 ± 0.2	$0.1(0.0 \text{ to } 0.1)$	1.1 ± 0.3	9	0.06-3.36	1
16	Br(9)	$19.1 \pm 1.9^{\text{d***}}$	$1.7(1.6 \text{ to } 1.8)$	1.1 ± 0.3	9	0.07-2.37	0.02
3	Et	$3.1 \pm 0.8^{***}$	$2.5(2.3 \text{ to } 2.5)$	1.1 ± 0.5	7	0.06-1.56	3.4
13	Br/Et	$4.9 \pm 1.3^{\text{d***}}$	$2.3(2.2 \text{ to } 2.4)$	1.6 ± 0.6	8	0.17-0.68	0.006
9	NH_2	$5.6 \pm 1.6^{***}$	$-0.7(-0.6 \text{ to } -0.8)$	1.0 ± 0.2	8	0.07-1.83	6.2
10	Br/ NH_2	$18.1 \pm 4.5^{\text{d***}}$	$1.7(1.7 \text{ to } 1.8)$	1.0 ± 0.2	7	0.07-2.64	0.02
	$\alpha 6\beta 4\text{I113A}$	$\text{EC}_{50}^{\text{a}}$	$\text{pEC}_{50} (\text{CI}_{95\%})^{\text{b}}$	Hill	n^{c}	$\text{Imax } \mu\text{A}$	Fold shift
1	Cytosine	3.1 ± 1.1	$-0.5(-0.3 \text{ to } -0.6)$	1.2 ± 0.4	7	0.05-19.10	1
16	Br(9)	$7.3 \pm 3.2^{\text{d***}}$	$2.1(2.0 \text{ to } 2.3)$	1.4 ± 0.7	7	0.07-1.34	0.003
3	Et	$0.8 \pm 0.2^{**}$	$0.1(0.0 \text{ to } 0.3)$	0.8 ± 0.2	5	0.20-14.07	0.25
13	Br/Et	$4.4 \pm 0.0^{\text{d***}}$	$2.4(2.2 \text{ to } 2.6)$	1.4 ± 0.3	4	0.07-11.52	0.0013
9	NH_2	$5.5 \pm 1.4^{**}$	$-0.7(-0.6 \text{ to } -0.8)$	1.0 ± 0.4	6	0.04-1.86	1.8
10	Br/ NH_2	$0.2 \pm 0.1^{***}$	$0.7(0.5 \text{ to } 1.3)$	0.8 ± 0.2	4	0.78-9.30	0.07
	$\alpha 6\beta 4\text{L121A}$	$\text{EC}_{50}^{\text{a}}$	$\text{pEC}_{50} (\text{CI}_{95\%})^{\text{b}}$	Hill	n^{c}	$\text{Imax } \mu\text{A}$	Fold shift

1	Cytisine	0.3±0.1	0.7(0.6 to 0.8)	2.1±0.8	8	0.18-17.23	1
16	Br(9)	13.6±8.5 ^{d**}	2.0(1.7 to 2.1)	1.6±0.6	7	0.19-27.22	0.03
3	Et	0.3±0.2	0.5(0.3 to 0.8)	1.0±0.5	8	0.12-6.95	1
13	Br/Et	14.2±3.2 ^{d***}	2.8(2.3 to 2.9)	1.0±0.7	6	0.12-6.77	0.03
9	NH ₂	23.5±4.5 ^{***}	-1.4(-1.3 to -1.5)	0.9±0.1	9	0.08-1.27	78.3
10	Br/NH ₂	0.1±0.0 ^{***}	1.0(0.9 to 1.1)	0.8±0.2	8	0.18-2.97	0.3

WT and mutated $\alpha 6\beta 4$ receptors were expressed in *Xenopus laevis* oocytes, and the potency of diverse cytosine derivatives with or without Br at the C(9) position were obtained. As above, the mRNA injection ratio was 10:1:5 corresponding to $\alpha 6\beta 4$:BARP. Dose response curves were monophasic and fitted to the Hill equation. Agonist EC₅₀ values are represented as mean \pm SD; fold shifts compared to cytosine. ^a ** p <0.01, *** p <0.001 compared to the corresponding cytosine EC₅₀, t-test; ^b pEC₅₀ corresponds to (-1*logEC₅₀); ^c corresponds to the number of cells; ^d EC₅₀ values in nM concentrations.

Table 5: The μM EC_{50} values and Hill coefficients for ACh and cytosine measured for WT and mutant $\alpha 6\beta 4$ receptors.

Receptor	Agonist	EC_{50} ^a	$\text{pEC}_{50} (\text{CI}_{95\%})$ ^b	Hill	n ^c	I_{max} μA	Fold shift
$\alpha 6\beta 4$	ACh	1.6 \pm 1.0	-0.2(-0.1 to -0.2)	1.2 \pm 0.7	11	0.12-7.77	1
TRPD-ALA	ACh	0.4 \pm 0.2**	0.4(0.4 to 0.5)	1.2 \pm 0.1	9	0.06-6.98	0.6
TYRC2-ALA	ACh	ND	ND	ND	7	ND	
TYRC2-PHE	ACh	3.1 \pm 1.1**	-0.5(-0.4 to -0.6)	1.2 \pm 0.6	9	0.07-4.94	2
TRPB-ALA	ACh	43.4 \pm 24.4***	-1.6(-1.5 to -1.7)	0.9 \pm 0.3	11	0.05-0.40	27
TYRA-ALA	ACh	12.9 \pm 3.1***	-1.1(-1.0 to -1.1)	0.7 \pm 0.2	6	0.29-5.89	8
Receptor	Agonist	EC_{50} ^a	$\text{pEC}_{50} (\text{CI}_{95\%})$ ^b	Hill	n ^c	I_{max} μA	Fold shift
$\alpha 6\beta 4$	Cytosine	0.5 \pm 0.2	0.3(0.2 to 0.3)	1.4 \pm 0.5	10	0.22-1.27	1
TRPD-ALA	Cytosine	0.3 \pm 0.1*	0.6(0.5 to 0.7)	1.5 \pm 0.1	7	0.06-1.55	0.5
TYRC2-ALA	Cytosine	ND	ND	ND	7	ND	
TYRC2-PHE	Cytosine	15.4 \pm 2.8***	-1.2(-1.1 to -1.2)	1.0 \pm 0.2	8	0.62-14.17	29
TRPB-ALA	Cytosine	3.8 \pm 0.9***	-0.6(-0.5 to -0.7)	0.6 \pm 0.1	10	0.07-0.71	7.2
TYRA-ALA	Cytosine	3.3 \pm 0.7***	-0.5(-0.4 to -0.6)	0.8 \pm 0.2	6	0.05-8.63	6.2

Key aromatic residues of the binding site, namely TRP-D, TYR-C2, TRP-B and TYR-A, were mutated to alanine and mutant receptors were expressed in *Xenopus laevis* oocytes. Agonist EC_{50} values are represented as mean \pm SD; fold shifts compared to ACh or cytosine accordingly. ^a * $p < 0.05$, ** $p < 0.01$, *** $p < 0.001$ compared to cytosine or ACh EC_{50} accordingly, t-test; ^b pEC_{50} corresponds to $(-1 * \log \text{EC}_{50})$; ^c corresponds to the number of cells.

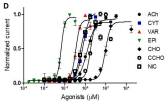
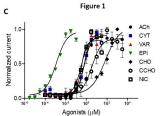
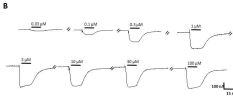
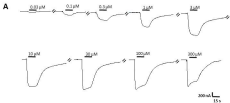


Fig. 2

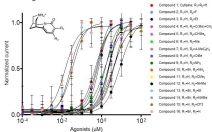


Fig. 3

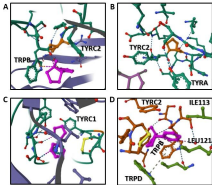
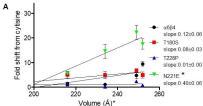


Figure 2



B

Sequence Alignment from Principal Binding Site Amino Acids

	Loop A	Loop B	Loop C
WAF4	WRPDI V L F	RTYDSRYV	SCCPDTF Y L D
Subunit	WTIPDI V L F	RTYDRAKI	SCCARE - I Y P D
a1 human	WRPDI V L F	RTYDRAKI	SCCARE - I Y P D
a2 human	WRPDI V L F	RTYDRAKI	SCCARE - I Y P D
a3 human	WRPDI V L F	RTYDRAKI	SCCARE - I Y P D
a4 human	WRPDI V L F	RTYDRAKI	SCCARE - I Y P D
a5 human	WRPDI V L F	RTYDRAKI	SCCARE - I Y P D
a6 human	WRPDI V L F	RTYDRAKI	SCCARE - I Y P D
a7 human	WRPDI V L F	RTYDRAKI	SCCARE - I Y P D
a8 human	WRPDI V L F	RTYDRAKI	SCCARE - I Y P D